

ASTE ^{12}CO ($J = 3-2$) Survey of Elliptical Galaxies

Hiroyuki NAKANISHI,¹ Tomoka TOSAKI,¹ Kotaro KOHNO,² Yoshiaki SOFUE,² and Nario KUNO¹

hnakanis@nro.nao.ac.jp

¹*Nobeyama Radio Observatory, Minamimaki, Minamisaku, Nagano 384-1305*

²*Institute of Astronomy, The University of Tokyo, 2-21-1 Osawa, Mitaka, Tokyo 181-0015*

(Received 2006 September 29; accepted 2006 November 27)

Abstract

We report on ^{12}CO ($J = 3-2$) observations of 15 nearby elliptical galaxies, carried out with the ASTE telescope. Thirteen were selected without regard to the presence of other tracers of cold interstellar matter. CO emission was detected from three of the galaxies, two of which were undetected by IRAS at $100\ \mu\text{m}$. The molecular gas masses range from 2.2×10^6 to $4.3 \times 10^8 M_{\odot}$. The ratio of the CO (3–2) and (1–0) lines, R_{31} , has a lower value for elliptical galaxies than for spiral galaxies, except for NGC 855, for which the value is close to the mean for spirals. The molecular gas in NGC 855 has a mean density in the range of $300\text{--}1000\ \text{cm}^{-3}$, adopting a temperature range of $15\text{--}100\ \text{K}$.

Key words: galaxies: elliptical — galaxies: ISM — ISM: molecules — radio lines: ISM

1. Introduction

Spiral galaxies contain substantial amounts of cold interstellar matter (ISM) and ongoing star formation, while cold ISM is but a minor component of elliptical galaxies. This is generally attributed to early exhaustion of the ISM in ellipticals during the early stages of galaxy formation. However, mass loss during stellar evolution (Faber & Gallagher 1976) can replenish the ISM to detectable levels in much less than a Hubble time, and ISM present in ellipticals can be attributed to stellar mass loss or to accretion from outside.

The mass loss from evolved stars is estimated to be $1.5 M_{\odot}$ per year per $10^{11} L_{\odot}$ of optical luminosity (Faber & Gallagher 1976), and is indeed observed to take place as cold molecular gas (e.g., Teyssier et al. 2006).

Thus, ISM contents comparable to those of spiral galaxies could be accumulated in elliptical galaxies on the order of 10^9 years. However, Knapp et al. (1985) pointed out that the cold gas and stellar contents of elliptical galaxies are uncorrelated, and concluded that the cold gas comes from outside, through events such as mergers. On the other hand, many elliptical galaxies contain on the order of 10^8 to $10^{10} M_{\odot}$ of hot gas, detected by X-ray emission (Forman et al. 1985), which could originate in collisionally-heated mass shed by dying stars (e.g., Mathews & Brighenti 2003).

Knowledge of the cold-gas content of normal elliptical galaxies is crucial regarding these questions. Several such surveys have been made (Lees et al. 1991; Sofue & Wakamatsu 1993; Wiklind et al. 1995; Knapp & Rupen 1996) using the CO (1–0) and CO (2–1) rotational lines as probes. However, all of these studies concentrated on ellipticals that were detected at $100\ \mu\text{m}$ by IRAS, and are therefore biased. The present paper discusses observations of 15 nearby elliptical galaxies selected independently of their infrared emission. These observations were made on the CO (3–2) line, which in addition to providing information on the presence of molecular gas, allows an evaluation of its physical condition from multi-transition

measurements (cf. Li et al. 1993; Vila-Vilaró et al. 2003).

2. Observations

We carried out ^{12}CO ($J = 3-2$) [hereafter CO (3–2)] observations of fifteen elliptical galaxies using the Atacama Submillimeter Telescope Experiment (ASTE), a 10 m antenna located at Pampa La Bola in the Atacama Desert of Chile at an altitude of 4800 m (Ezawa et al. 2004; Kohno 2005). The observations were made on 2006 August 21–24 from a remote ASTE operations room at the Nobeyama Radio Observatory (NRO) using the network operation system N-COSMOS 3, developed at the National Astronomical Observatory of Japan (NAOJ) (Kamazaki et al. 2005). The front end is a cartridge-type 350 GHz receiver operated in the double-sideband mode with an intermediate frequency (IF) of between 5 and 7 GHz. The antenna temperature and sky the extinction were measured using the standard chopper-wheel method. The antenna beam size was $22''$ at 345 GHz. We used three digital spectrometers with a bandwidth of 512 MHz ($445\ \text{km s}^{-1}$ at 345 GHz) and 1024 channels. The same center frequency was set for these spectrometers. The velocity resolution was $0.53\ \text{km s}^{-1}$. The pointing was monitored by observations of the bright line sources AFGL 3068 and σ Ceti, and was accurate to $5''$. The main beam efficiency, η_{MB} , was measured each day by observations of W 51D using the peak intensity measured by Wang et al. (1994), which was constant at 0.54.

The observed galaxies were selected from a catalogue of Knapp et al. (1989) to lie in the right ascension range $22^{\text{h}}\text{--}7^{\text{h}}$ and between declinations of $-30^{\circ}\text{--}+20^{\circ}$ (so that the galaxies could be observed from both the Northern and Southern hemispheres), to have recession velocities less than $5000\ \text{km s}^{-1}$ and to be classified as ellipticals, rather than as S0s or of later types. No other criterion was used for thirteen of the galaxies, so they are unbiased. In addition, two infrared-bright dwarf ellipticals, NGC 855 and NGC 2328, were observed. In these galaxies, CO (1–0) and CO (2–1) emissions were observed;

Table 1. Target list.*

Name	RA(B1950)			Dec(B1950)			Morphology	B_T mag	$V_{\text{HEL-OPT}}$ km s ⁻¹
	h	m	s	°	'	''			
First samples									
NGC 596	01	30	22	-07	17	18	E1	11.8	1817
NGC 636	01	36	36	-07	45	54	E3	12.4	1805
NGC 821	02	05	41	+10	45	32	E6	11.7	1716
NGC 990	02	33	36	+11	25	28	E	13.9	3508
NGC 1453	03	43	57	-04	07	36	E2	12.6	3906
NGC 1550	04	17	02	+02	17	25	E	14.0	3689
NGC 1600	04	29	12	-05	11	30	E4	12.0	4687
NGC 7458	22	58	55	+01	29	05	E	13.9	4981
NGC 7464	22	59	25	+15	42	17	E1p	—	1877
NGC 7468	23	00	30	+16	20	08	E3p	14.0	2089
NGC 7619	23	17	43	+07	55	57	E2	12.3	3747
NGC 7626	23	18	10	+07	56	35	E	12.3	3450
NGC 7785	23	52	45	+05	38	11	E5	12.6	3826
Second samples									
NGC 855	02	11	10	+27	38	36	E	13.3	600
NGC 2328	07	01	01	-41	59	42	E/S0	13.3	1159

* These parameters are taken from Knapp et al. (1989).

the line widths were less than 445 km s⁻¹. The observed galaxies are listed in table 1.

Data reduction was carried out with tasks in NEWSTAR, a package developed at NRO. Individual bad data were flagged, the remaining spectra averaged, and first-order baselines were removed. The calibrated spectra were smoothed by 46 channels to a velocity resolution of 19.8 km s⁻¹. The typical rms noise levels, ΔT_{MB} , for the smoothed spectra were 8 mK.

3. Results

3.1. Spectra

The spectra for all fifteen observed galaxies are shown in figure 1 and the observational quantities are listed in table 2. We detected CO (3–2) emission from three galaxies, all for the first time [the observation of NGC 855 by Vila-Vilaró et al. (2003) was not sufficiently sensitive to detect emission at the level of that measured in here].

The spectrum for NGC 1550 is highly asymmetric relative to the systemic velocity measured in optical observations. In order to examine whether this detection is real, we halved the original data into two independent groups, and then averaged the spectra belonging to each one. In both cases, similar profiles were obtained, as shown in figure 2. Hence, we can conclude that this detection is likely to be real.

Although the IRAS 100 μm flux in NGC 7464 is the highest in our observed sample, CO emission was not detected (Wiklind et al. 1995). NGC 7468 was detected in only the CO (1–0) line at 22'' beam (Wiklind et al. 1995), which is the same as our observing beam size. Since the CO (1–0) peak temperature is about 20 mK, the CO (3–2) peak temperature would be about 4 mK, assuming the mean line ratio for elliptical galaxies to be $R_{31} = 0.21$ (Vila-Vilaró et al. 2003). The rms noise

of 7 mK in our observation was not low enough to detect CO (3–2) emission.

Although NGC 2328 was detected in both the CO (1–0) and (2–1) lines (Wiklind et al. 1995; Lees et al. 1991), we could not detect CO (3–2) emission. The peak temperature of the CO (1–0) line was about 15 mK for a 44'' beam. If the size of the molecular distribution was less than 22'', and if the R_{31} was 0.21, the CO (3–2) peak temperature would be about 13 mK. The rms noise in our observation was too high (12 mK) to detect the line.

Note that CO (3–2) emission could not be detected if the velocity width was larger than the bandwidth of the spectrometers (445 km s⁻¹).

3.2. Molecular Masses

We assumed an average ratio, R_{31} , of 0.21 to estimate the expected CO (1–0) flux for two of the galaxies, and used the CO (1–0) data for NGC 855 from Wiklind et al. (1995). The molecular hydrogen mass was calculated from

$$M_{\text{H}_2} = \frac{\pi}{4} X_{\text{CO}} \frac{I_{\text{CO}(3-2)}}{R_{31}} m_{\text{H}_2} \theta^2 d^2. \quad (1)$$

The distance was calculated from the recession velocity, V , assuming a Hubble constant of 72 km s⁻¹ Mpc⁻¹ (Spergel et al. 2003). The conversion factor was taken to be $X_{\text{CO}} = 2.8 \times 10^{20} \text{ cm}^{-2} \text{ K}^{-1} \text{ km}^{-1} \text{ s}$, the average of the values found for nearby Galactic molecular clouds by Arimoto et al. (1996). The resulting masses are listed in table 3, and cover a similar range as those measured for other elliptical galaxies (Lees et al. 1991; Sofue & Wakamatsu 1993; Wiklind et al. 1995).

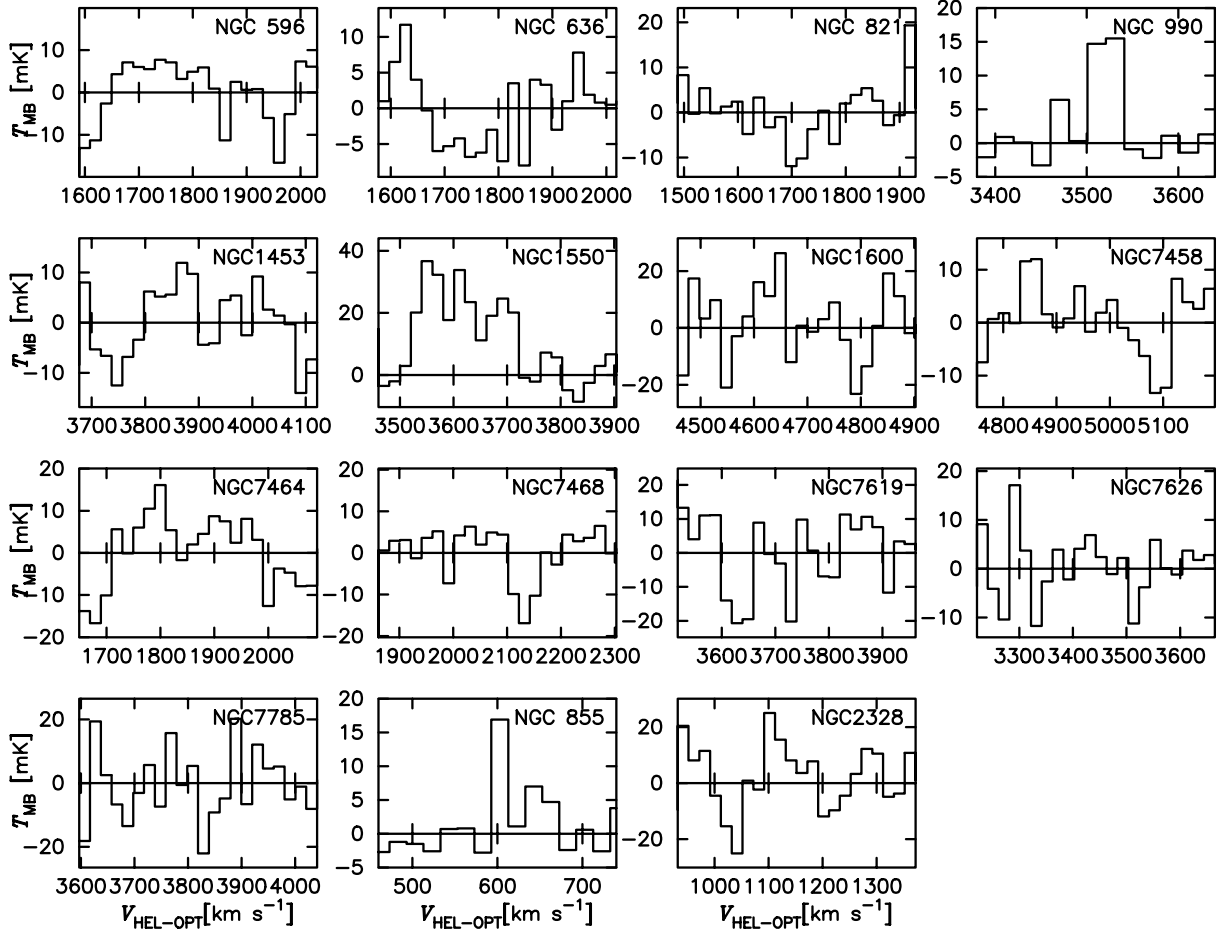


Fig. 1. CO spectra of all the observed elliptical galaxies.

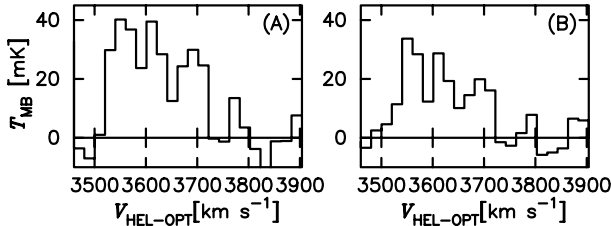


Fig. 2. Spectra for NGC 1550. We halved the original data into two independent groups. Presented spectra were obtained by averaging the spectra belonging to the individual groups.

4. Discussion

4.1. Line Ratios for NGC 855

Both the CO(1–0) and CO(2–1) emissions were detected from NGC 855 (Lees et al. 1991; Wiklind et al. 1995). Comparisons with the observations of Wiklind et al. (1995) gives line ratios of $R_{31} = 0.5$ and $R_{21} = 0.8$. The beam sizes used for the CO(3–2) and CO(1–0) were the same, $22''$, while the beam size for the CO(2–1) observation was $11''$. Therefore, the true value of R_{21} might be a factor 1 to 4 lower, while R_{31} can be considered to be the true value.

The value of R_{31} is larger than the mean observed for

three other elliptical galaxies (0.2, Vila-Vilaró et al. 2003), but similar to values observed for spiral and starburst galaxies (Mauersberger et al. 1999).

4.1.1. Star formation efficiency

The star formation efficiency (SFE) of NGC 855 is about $8 \times 10^{-10} \text{ yr}^{-1}$ (Vila-Vilaró et al. 2003), higher than that of most elliptical galaxies, and similar to values observed for spiral galaxies (Komugi et al. 2005). This suggests that R_{31} correlates with the star-formation efficiency, as noted from mapping of M 83 by Muraoka and Kohno (2006) and Muraoka et al. (2006).

4.1.2. Modeling the molecular ISM

Since we had data for three CO rotational in NGC 855, the mean properties of the molecular ISM could be modelled. First, we assumed LTE, and that all three CO lines are optically thick. The brightness temperature, T_b , is then

$$T_b = \frac{h\nu}{k} \left\{ \left[\exp\left(\frac{h\nu}{kT}\right) - 1 \right]^{-1} - \left[\exp\left(\frac{h\nu}{2.7k}\right) - 1 \right]^{-1} \right\}, \quad (2)$$

where h is Planck's constant, ν is frequency, k is Boltzmann's constant, and T is the kinetic temperature. Applying equation (2) to the observed line ratios for NGC 855 implies a kinetic temperature of 8 K, which is far lower than the dust temperature of 33 K estimated by Wiklind et al. (1995).

Table 2. Observational quantities.*

Name	$F_{100\mu\text{m}}$ Jy	V_{CO} km s^{-1}	ΔV_{CO} km s^{-1}	T_{peak} mK	I_{CO} K km s^{-1}	ΔT_{MB} mK	Comment
(1)	(2)	(3)	(4)	(5)	(6)	(7)	(8)
First samples							
NGC 596	≤ 0.300	—	—	8	—	8	no detection
NGC 636	≤ 0.399	—	—	12	—	5	no detection
NGC 821	0.440	—	—	19	—	6	no detection
NGC 990	≤ 2.24	3531	40	16	0.59	3	detection
NGC 1453	0.670	—	—	12	—	7	no detection
NGC 1550	≤ 0.651	3631	198	37	4.9	5	detection
NGC 1600	0.170	—	—	26	—	15	no detection
NGC 7458	≤ 0.192	—	—	12	—	8	no detection
NGC 7464	6.71	—	—	16	—	8	no detection
NGC 7468	1.65	—	—	7	—	7	no detection
NGC 7619	0.630	—	—	13	—	11	no detection
NGC 7626	≤ 0.339	—	—	17	—	7	no detection
NGC 7785	≤ 0.264	—	—	20	—	11	no detection
Second samples							
NGC 855	3.27	613	20	17	0.36	4	detection
NGC 2328	3.77	—	—	25	—	12	no detection

* (1) Galaxy name. (2) IRAS $100\mu\text{m}$ flux. The upper limit was taken to be 3σ . (3) Central velocity. (4) Velocity width (full width at zero intensity: FWZI). (5) Peak brightness temperature. (6) Integrated intensity. (7) Rms noise. (8) Comment on detection.

Table 3. Inferred properties of molecular gas.

Name	M_{H_2} M_{\odot}	Volume pc^3	Diameter pc
NGC 990	2.7×10^8	(8.3×10^6)	(250)
NGC 1550	4.3×10^8	(1.3×10^7)	(300)
NGC 855	2.2×10^6	6.9×10^4	(51)

Accordingly, we modelled the emission using the Large Velocity Gradient (LVG) model (Goldreich & Kwan 1974). We calculated line ratios for kinetic temperatures from 10–100 K, H_2 densities from 10 to $6.3 \times 10^6 \text{ cm}^{-3}$, and CO abundances, $X_{\text{CO}}(dV/dr)^{-1}$, of 10^{-6} , 10^{-5} , and $10^{-4} \text{ pc km}^{-1} \text{ s}$. The resulting line ratios, R_{31} and R_{21} , are shown in figure 3. The data and models match well for $T > 15 \text{ K}$, compatible with the dust temperature. The corresponding density is in the range of $300\text{--}1000 \text{ cm}^{-3}$. The CO (1–0) line is optically thick at this density, as was assumed in estimating the molecular mass from equation (1).

4.2. Volume and Size of Molecular Distribution

Using the calculated mean density, we could estimate the volume of the molecular gas and its diameter, assuming a spherical distribution. We used a mean H_2 density of 650 cm^{-3} for all three detected elliptical galaxies. The results are given in table 3. The molecular content in NGC 855 is as much as a single Galactic Giant Molecular Cloud (GMC), which can support the existence of the star formation in this galaxy (e.g.,

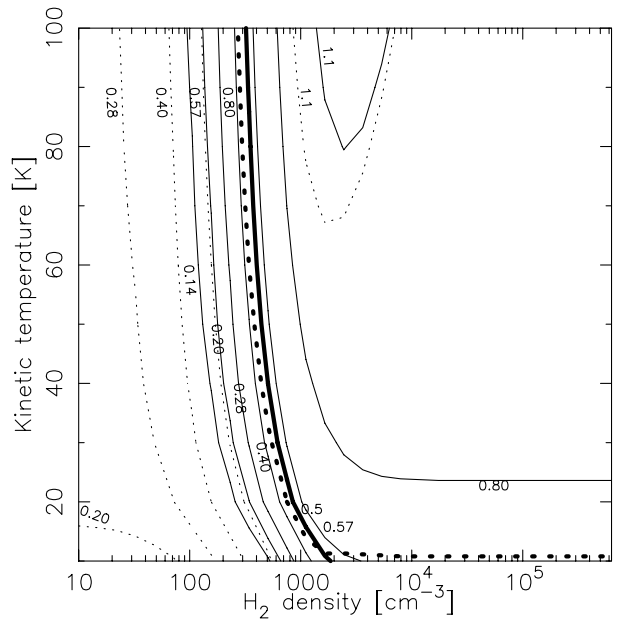


Fig. 3. Results of LVG calculations, adopting a CO abundance of $X_{\text{CO}}/(dV/dr) = 10^{-5} \text{ pc km}^{-1} \text{ s}$. The solid and dotted lines denote R_{31} and R_{21} , respectively. The thick solid and dotted lines denote $R_{31} = 0.5$ and $R_{21} = 0.8$, respectively.

Vila-Vilaró et al. 2003).

However, the size is smaller than the beam size of CO (2–1) ($11''$), which corresponds to 440 pc at 8.3 Mpc . Therefore, R_{21} would be 4-times smaller (i.e., $R_{21} = 0.2$), if NGC 855 had only

one GMC. The LVG calculation cannot satisfy $R_{31} = 0.5$ and $R_{21} = 0.2$ at the same time, if this was the case. The curve of $R_{31} = 0.5$ always coincides with that of $R_{21} \sim 0.8$.

Considering these matters, the molecular distribution is likely to be more extended than the beam size $22''$, forming smaller clumps, rather than one GMC.

4.3. Comparison with IRAS Fluxes

Two of the elliptical galaxies (NGC 990 and NGC 1550) in which we detected molecular gas were not detected by IRAS, even though the IRAS $100\ \mu\text{m}$ upper limit of NGC 990 is fairly high. Thus, cold molecular ISM may well be present in more ellipticals than previously thought.

5. Summary

We achieved a ^{12}CO ($J = 3-2$) line survey of 15 elliptical galaxies, and confidently detected CO emissions from three ellipticals. The molecular gas masses were estimated to be $2.2 \times 10^6 - 4.3 \times 10^8 M_{\odot}$.

The line ratio, R_{31} , of NGC 855 was calculated to be 0.5.

We performed a line ratio analysis using R_{31} and R_{21} of NGC 855. The LVG model showed that the H_2 density was $3 \times 10^2 - 1 \times 10^3\ \text{cm}^{-3}$ in the temperature range of 15–100 K.

CO ($J = 3-2$) emission was detected even in ellipticals, which are undetected by IRAS at $100\ \mu\text{m}$.

We are grateful to all of the ASTE staff for their dedicated support during our observations. We thank the referee Dr. Knapp for substantial corrections of English as well as invaluable scientific comments, which greatly improved our paper. We thank Dr. T. Sawada and Dr. S. Takano for fruitful discussions and advice concerning the observations. This study was financially supported by the MEXT Grant-in-Aid for Scientific Research on Priority Areas No. 15071202. Observations with ASTE were in part carried out remotely from Japan by using NTT's GEMnet2 and its partner R&E (Research and Education) networks, which are based on AccessNova collaboration of University of Chile, NTT Laboratories, and National Astronomical Observatory of Japan.

References

- Arimoto, N., Sofue, Y., & Tsujimoto, T. 1996, PASJ, 48, 275
 Ezawa, H., Kawabe, R., Kohno, K., & Yamamoto, S. 2004, Proc. SPIE, 5489, 763
 Faber, S. M., & Gallagher, J. S. 1976, ApJ, 204, 365
 Forman, W., Jones, C., & Tucker, W. 1985, ApJ, 293, 102
 Goldreich, P., & Kwan, J. 1974, ApJ, 189, 441
 Kamazaki, T., et al. 2005, ASP Conf. Ser., 347, 533
 Knapp, G. R., Guhathakurta, P., Kim, D.-W., & Jura, M. A. 1989, ApJS, 70, 329
 Knapp, G. R., & Rupen, M. P. 1996, ApJ, 460, 271
 Knapp, G. R., Turner, E. L., & Cunniffe, P. E. 1985, AJ, 90, 454
 Kohno, K. 2005, ASP Conf. Ser., 344, 242
 Komugi, S., Sofue, Y., Nakanishi, H., Onodera, S., & Egusa, F. 2005, PASJ, 57, 733
 Lees, J. F., Knapp, G. R., Rupen, M. P., & Phillips, T. G. 1991, ApJ, 379, 177
 Li, J. G., Seaquist, E. R., & Sage, L. J. 1993, ApJ, 411, L71
 Mathews, W. G., & Brighenti, F. 2003, ApJ, 599, 992
 Mauersberger, R., Henkel, C., Walsh, W., & Schulz, A. 1999, A&A, 341, 256
 Muraoka, et al. 2006, PASJ, 59
 Muraoka, K., & Kohno, K. 2006, IAU Symp., 237, 173
 Sofue, Y., & Wakamatsu, K.-I. 1993, PASJ, 45, 529
 Spergel, D. N., et al. 2003, ApJS, 148, 175
 Teyssier, D., Hernandez, R., Bujarrabal, V., Yoshida, H., & Phillips, T. G. 2006, A&A, 450, 167
 Vila-Vilaró, B., Cepa, J., & Butner, H. M. 2003, ApJ, 594, 232
 Wang, Y., Jaffe, D. T., Graf, U. U., & Evans, N. J., II 1994, ApJS, 95, 503
 Wiklind, T., Combes, F., & Henkel, C. 1995, A&A, 297, 643